

SURFACE-LAYER RESPONSE TO TOPOGRAPHIC SHADING IN MIERS VALLEY, ANTARCTICA

Marwan Katurji^{1,2,*}, Peyman Zawar-Reza¹, Shiyuan Zhong²

¹Centre for Atmospheric Research, University of Canterbury, Christchurch, New Zealand

²Department of Geography, Michigan State University, East Lansing, MI, USA

[*marwan.katurji@canterbury.ac.nz](mailto:marwan.katurji@canterbury.ac.nz)

1. INTRODUCTION

In this study, we investigate transitional surface-layer in response to topographic shading using observational data from Miers Valley, which is situated within the McMurdo Dry Valley system (Figure 1). To our knowledge, this is the first attempt at describing mean and turbulent flow characteristics throughout the depth of the atmospheric surface layer (up to 250 m AGL) within the Dry Valley system. Although the observational period is short (9 days), this dataset presents a rare insight into the summertime valley atmosphere and provides a unique opportunity for investigating the dynamics of flow in a transitioning state – in this case, due to topographic shading. Particular focus will be placed on defining the sensitivity of the valley atmosphere to topographic shading and how that reflects on the surface energy balance, near surface temperature, and low frequency oscillations in the 3-dimensional velocity field.

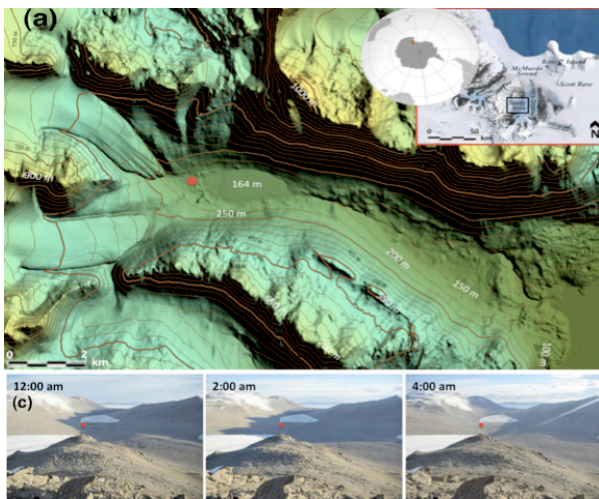


Figure 1. Map of the area showing the shading characteristics.

Shading due to terrain obscuring the incoming solar radiation can have implications to the microclimate variability on the shaded region. Whiteman et al. (1989) showed that valley floor shading could cause variations in observed meteorological fields within the same valley and can scale to or surmount the variations measured at one site. Topographic shading could also delay

(speed up) temperature inversion breakup (buildup) within valleys as shown through the numerical simulations of Colette et al. (2003).

Topographic shading for extended periods of time can be similar to early evening transition (EET) periods due to the decrease and eventual extinction of solar radiation. Previous studies have examined the surface layer dynamics associated with the EET, but exact onset time of EET can be complicated by the presence of topographic shading in areas of complex terrain. Mahrt (1981) defines the onset of EET as when the surface-layer winds (within a height of 100 m) start to decelerate 2 hours prior to sunset, while the total period of the EET can take up to 4 or 5 hours. Busse and Knupp (2012) showed that the 10 m winds can start to decrease 30 minutes before sunset, while it takes another 2.5 hours for EET to manifest throughout the depth of the boundary layer.

The theoretical and laboratory work by Hunt et al. (2003) identified specific dynamics of flow transition over gentle and long (5 to 15 km) slopes. Their work highlighted that the transition over gentle slopes occurs over a period of several (1 to 4) hours, and the length of the period is proportional to the depth of the convective boundary layer and inversely proportional to the speed of the upslope flow. The EET, following Hunt et al. (2003), occurs within a layer of 10 to 100 m above the surface and is initiated by a transitional downward propagating front triggered at a location upslope where the upward flow momentum is counteracted by the negative buoyancy caused by the surface cooling. The reversal of the flow from anabatic (upslope or up valley) to katabatic (downslope or down valley) can occur at a variety of time and length scales depending on slope angle, pre-exposure to solar radiation, and elevation.

2. PHYSICAL SETTING AND CLIMATE

The northward migration of the circumpolar trough in the summer season generates weak synoptic pressure gradients over the Ross Sea region. As a result, large-scale surface winds are generally weak over the Dry Valley area, allowing for the predominance of thermally driven circulations. The observational period, which

occurred in January of 2012, was within this typical summertime weather regime.

The surface climatology of the winds of the Dry Valleys has been studied extensively in the past, and continues to be of interest under climate change. Summertime conditions allow for anabatic (up valley and upslope) and katabatic (down valley and down slope) diurnal oscillations whenever the synoptic pressure gradients are weak (McKendry and Lewthwaite 1992; Doran et al. 2002; Nylén et al. 2004). Little is known about boundary layer structure and winds in smaller valley systems (Garwood, Marshall, Miers and Hidden Valley).

Miers Valley is one of the smaller Dry Valley systems; the north and south mountain slopes have mean slope angles varying between 15° and 25°. The valley's elevation drops east of the lake towards the Ross Sea along a declining slope of around 3 to 5 degrees (Figure 1).

An observational campaign was carried out for a 9-day period (January 13 to 22, 2012) in which surface and atmospheric boundary-layer measurements were taken. Two systems were deployed; first is a sound detection and ranging (SODAR) profiler for measuring 3D boundary-layer wind components from the surface up to a height of 500 m at 5 m intervals and 10-minute averages. The SODAR was located in the upper Miers Valley to the east of the frozen Lake Miers (Figure 1). The second is a 2m micrometeorological flux tower equipped with a 3D sonic anemometer and an infrared moisture analyzer for measuring turbulent momentum, heat and moisture fluxes and a net-radiometer. Soil temperatures were also taken at 2 and 25 cm below the surface for measuring ground heat fluxes.

3. DATA PROCESSING

The sonic anemometer's sampling frequency was at 60 Hz, which was block averaged to 20 Hz by the signal-processing unit. The data set (from the eddy-covariance system and SODAR) was run through an outlier removal algorithm and filtered for erroneous data. The sonic anemometer turbulence measurements (at 20 Hz sampling resolution) were rotated according to Wilczak et al. (2001) to eliminate any constructional tilt in the sonic anemometer plane that would lead to biases, especially in the vertical fluxes.

When deriving the turbulent fluxes an averaging interval should be chosen, if one uses a large enough interval, on the order of 1 hour or more, then the analysis would have an inherent feature of filtering out any smaller scale variability. This is essential in the case of investigating transitional flows that could have turbulent time response less than 10 s (Mahrt and Vickers 2006), or reaction times to an external forcing on the

order of 30 to 120 s (Kossman and Feidler 2000). In this study we have chosen to use a 10-minute averaging interval for surface turbulent flux calculations based on the finding that periods of 1 to 30-minute did not produce significant differences.

Soil and air temperatures and radiative fluxes (incoming and outgoing short and long-wave radiation) were sampled at 1 Hz. To calculate soil heat flux, soil conductivity is needed, and to our knowledge soil conductivity measurements have not been made for the Dry Valley soils. So a range of values was used based on measured soil conductivity from the literature from regions around Antarctica, including Scott Base soils.

The extremely dry air lowered the SODAR range from a set value of 500 m to 100-300 m. The very low atmospheric moisture in the Dry Valley boundary layer affected the quality of the SODAR data. On average, the maximum reliable height range below which data were collected was 250 m. Data availability was 80% for range heights up to 50 m, and then a drop to 60% for levels above 50 and 100 m.

4. RESULTS AND DISCUSSION

At this site, the period of shade during the month of January extends from 00:00 LST to around 04:00 LST. Surface energy balance has been studied routinely around Antarctica, but mainly over snow and ice where mass balance of the snow is the point of interest (Van As et al. 2005; Van den Broeke et al. 2006). The objective of this study is to understand the drivers of the transitional period and the evolution of the terms in the surface energy budget.

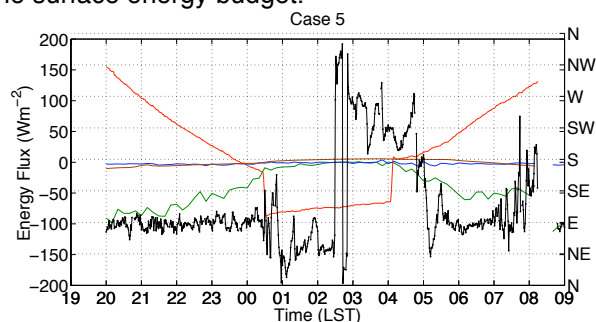


Figure 2. 10-minute averaged net-radiative flux (red line), ground heat flux (brown line), latent heat flux (blue line), sensible heat flux (green line), and wind direction (black line).

We focused on the five cases over which the transition from a non-shaded convective unstable boundary layer to a shaded stable boundary layer took place, only one case is shown in Figure 2. As soon as the shade is cast, the incoming solar radiation drops to zero and the surface starts to cool as net radiative flux attains negative values (-75 Wm^{-2}). The changes in the ground and latent

heat fluxes are very small compared to the sensible heat flux and net-radiative flux. The sensible heat flux approaches zero, but there is a delayed response of sensible heat flux to the shade because of momentum and thermal inertia due to the decaying surface eddies.

After the onset of the shade, the soil surface temperatures dropped by around 8 to 10 °C (Figure 3); this is similar in magnitude to the drop observed by vegetated steep alpine slopes in the mid-latitudes (Nadeau et al. 2012). The air temperatures did not drop as sharp as the soil surface temperature, and only exhibited a decrease of about 2 °C. The difference between the rate of decrease of soil surface temperatures and air temperatures may be attributed to the fact that soil surface temperature responds directly to the changes in radiative forcing, but air temperature responds to radiative forcing primarily through turbulent mixing.

A careful examination of the soil surface temperature time series reveals two time scales at which the temperature decreases: a short time scale of about one hour (between 00:30 and 01:30 LST in Figure 3) immediately following the onset of the shade during which the temperature drops rapidly, and a longer time scale during which temperature continues to drop at a near linear rate until the shade passes. The exponential decrease can be significantly reduced by the presence of cloud cover, which happened in other cases.

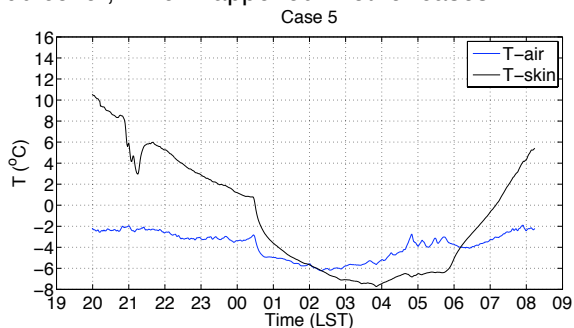


Figure 3. Time evolution of the air and soil surface or skin temperature.

Wind direction derived from the sonic anemometer horizontal velocity components during the shade period is shown in Figure 2. The persistent easterly wind direction during the non-shade period of the day becomes intermittent and oscillates as soon as the shade is cast. Long wavelength oscillations appear, and are superimposed on the easterly direction. This oscillatory horizontal wind directional shear persists for 2 to 3 hours, but does not develop in all cases. Subsequently, winds transition to a northerly regime and then to south southwesterly regime representing downslope flows or flows from the glaciers lying west of the measurement station.

SODAR wind speed and direction composites averaged over a 2-hour period for the entire sampling time are shown in Figure 4. The non-shade periods of the day are associated with steady wind speeds between 4 and 4.8 ms^{-1} throughout from surface to 110 m AGL. These winds have minimum directional shear and are primarily up-valley. They also exhibit a weak jet at around 60 m AGL.

During the transition period and into the shade time (00:00 to 04:00 LST) winds decelerate to as low as 2 ms^{-1} . Directional shear increases as the surface decouples from the upper-level winds causing a clockwise rotation with height. The upper-level directional shear could be a result of more buoyant (warmer) downslope or down glacier flows that override the cold pool established on the valley floor and flows on top of it. The evidence from the SODAR data does show a varying valley boundary layer that responds to topographic shading. The transition appears to be felt throughout the valley boundary layer and up to heights of at least 250 m AGL.

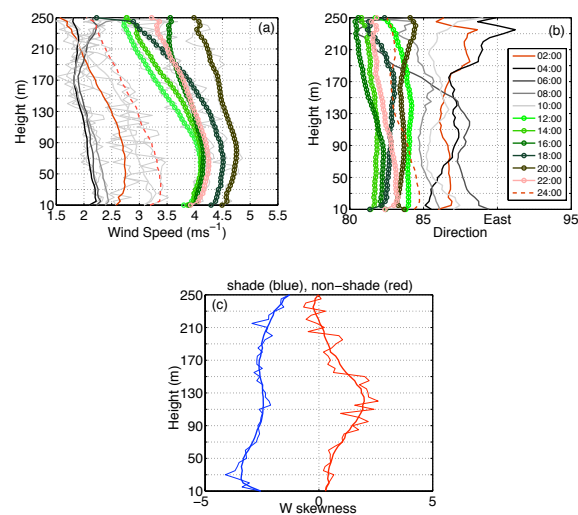


Figure 4. Composite average of 9 days for 2-hour bins of (a) wind speed and (b) direction vertical profiles measured by the SODAR and vertical velocity skewness out of 715 data points for shade time and 869 for non-shade time (c). The blue line shows the composite average of the periods between 00:00 to 04:00 LST while the red line shows the average for periods outside this time.

Atmospheric stability can be derived from wind turbulent statistics stored by SODAR, and be used to assess static stability in absence of temperature profiles. The vertical velocity (w) third-order moments or triple correlations represent the vertical transport of vertical momentum by turbulence, statistically represented with vertical velocity skewness, will reflect the mode of eddy transport within the boundary layer. Positive velocity skewness that increases with height, which is a result of upward transfer of turbulent

motion by ascending eddies, should represent a well-mixed boundary layer. The opposite applies when the ground cools and eddies tend to transport turbulence towards the surface, leaving a negative vertical velocity skewness decreasing or not changing with height; this represents a stable boundary layer. Atmospheric boundary layer stability and cloud tops and inversions have been previously analyzed using vertical velocity skewness variations instead of vertical temperature profiles (Moeng and Rottuno 1990). Figure 4c shows the vertical velocity skewness profile averaged for both non-shade and shade periods. From these results it is apparent that topographic shading can modify atmospheric stability throughout the depth of the valley boundary layer. This is indicated by negative vertical velocity skewness throughout a 250 m deep layer. There appears to be a strong gradient 10 to 20 m above ground level, which could be associated with the stronger atmospheric stability. During the non-shaded period there is a positive velocity skewness that produces an inflection point at round 120 m AGL. The 120 ± 20 m AGL marks the height of the daytime well-mixed boundary layer. Above this height the horizontal wind speeds start decreasing with height.

used in the decomposition; bright and dark colors are high and low magnitudes respectively.

To examine the time evolution of the frequency of the measured wind velocities, wavelet transform is used. Wavelets are used to examine the low frequency evolution of the flow structure as the valley flow transitions into the stable regime. Particular interest will be put in depicting oscillations that occur during the transitional flow. The wavelet analysis uses the de-trended time series of the 1-minute sampled velocity components and it is applied over a 13-hour period centered on the time of shade onset. A continuous wavelet transform is used; the selected mother wavelet is the Morlet wavelet, which has been applied successfully to atmospheric boundary layer analysis.

Figure 5 shows the time evolution of the periodicity or frequency in the time series of the u and v velocity components. Interesting oscillations appear after the onset of the shade time (00:00 LST). These are measured by the presence and absence of high magnitude (bright colors) pulses. The along valley wind component (u) appears to transition into a high-period wave (~ 60 minutes between 00:00 and 02:30 LST) and then into a low-period one (~ 25 minutes between 02:30 and 04:00 LST) and then back again into a high period wave after 04:00 LST. On the other hand, the cross-valley wind component (v) transitions into a low period wave after 00:00 LST with a gradual shift into a longer oscillatory wave period between 35 and 60 minutes. The vertical wind velocity wavelet transform (not shown) resembles the u wind component oscillations. These results show the dynamics of flow deceleration, stagnation and oscillations as the adjusts from an unstable to a stable boundary layer. The large air mass comes up-valley and scales to the longer terrain fetch, and as the shade is cast over the valley, retains some of the longer wavelengths of the flow and decelerates accordingly. The smaller air mass originating from the slopes appears to be quicker to adjust to low-period oscillations and takes about 3 more hours before it ties in with the oscillatory pattern of the up-valley flow.

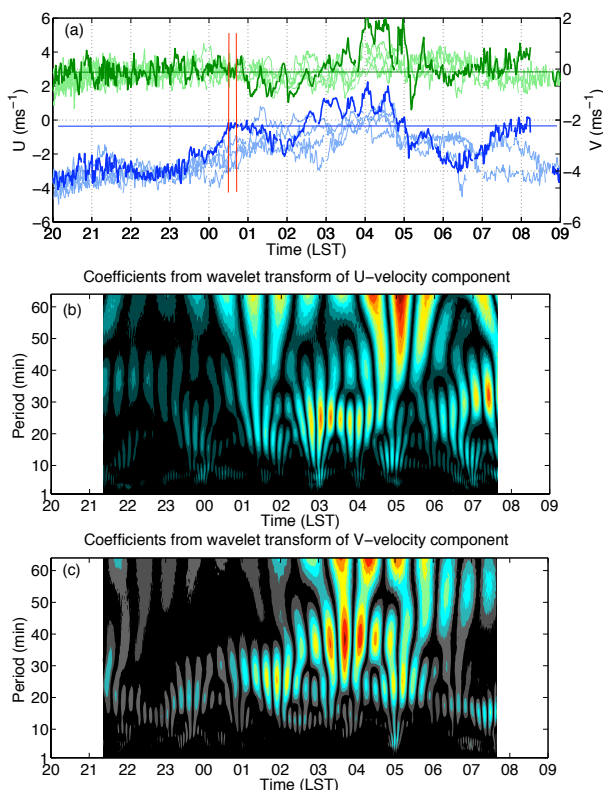


Figure 5. (a) Time series of u -velocity component (along valley, blue line) and v -velocity (cross valley, green line) for the 5 cases of shade periods over the 13-hour period centered over the shade cast time (00:00 LST). Bold lines represent case 5 (bottom two panels of Figure 3). (b) and (c) represent the wavelet transform of the u and v -velocity components. Shaded contours are the coefficients of the wavelets

5. ACKNOWLEDGEMENTS

The authors wish to thank Antarctic New Zealand for providing logistical support for this research. Also the nzTABS programme under which this campaign was carried out.

6. REFERENCES

- Busse, J., and K., Knupp, 2012: Observed characteristics of the afternoon-evening boundary layer transition based on sodar and surface data, *J. Appl. Meteorol. Clim.*, **51**, 571–582.
- Colette, A., F. K. Chow, and R. L. Street, 2003: A numerical study of inversion-layer breakup and the effects of topographic shading in idealized valleys, *J. Appl. Meteorol.*, **42**, 1255-1272.
- Hunt, J. C. R., Fernando, H. J. S., and M. Princevac, 2003: Unsteady thermally driven flows on gentle slopes, *J. Atmos. Sci.*, **60**, 2169-2182.
- Doran, P. T., McKay, C. P., Clow, G. D., Dana, G. L., Fountain, A. G., Nylén, T., and W. B. Lyons, 2002: Valley floor climate observations from the McMurdo dry valleys, *J. Geophys. Res.*, **107**, 1-12.
- Kossman, M., and Fiedler, F., 2000: Diurnal momentum budget analysis of thermally induced slope winds, *Meteorol. Atmos. Phys.* **75**, 195-215.
- Mahrt, L., 1981: The early evening boundary layer transition, *Q. J. Roy. Meteorol. Soc.*, **554**, 329-343.
- Mahrt, L., and D. Vickers, 2006: Extremely weak mixing in stable conditions, *Bound.-Layer Meteor.*, **119**, 19-39.
- McKendry, I., and E. Lewthwaite, 1992: Summertime along-valley wind variations in the Wright Valley Antarctica, *Int. J. Climatol.*, **12**, 587–596.
- Moeng, C. H., and R. Rotunno, 1990: Vertical-velocity skewness in the buoyancy driven boundary layer, *J. Atmos. Sci.*, **47**, 1149-1162.
- Nadeau, D. F., Pardyjak, E. R., Higgins, C. W., Huwald, H., and M. B. Parlange, 2012: Flow during the evening transition over steep Alpine slopes, *Q. J. R. Meteorol. Soc.*, DOI:10.1002/qj.1985.
- Nylén, T. H., Fountain, A. G., and P. T. Doran, 2004: Climatology of katabatic winds in the McMurdo dry valleys, *J. Geophys. Res.*, **109**, 1-9.
- Van As, D., Van den Broeke, M., and R., Van de Wal, 2005: Daily cycle of the surface layer and energy balance on the high Antarctic Plateau, *Antarct. Sci.*, **17**, 121-133.
- Van den Broeke, M., Reumer, C., Van As, D., and W., Boot, 2006: Daily cycle of the surface energy balance in Antarctica and the influence of clouds, *Int. J. Climatol.*, **26**, 1587-1605.
- Whiteman, C. D., Allwine, K. J., Fritschen, L. J., Orgill, M. M. and J. R. Simpson, 1989: Deep valley radiation and surface energy budget micro-climates. Part I: Radiation, *J. Appl. Meteorol.*, **28**, 414-426.
- Wilczak, J., Oncley, S., and S. Stage, 2001: Sonic anemometer tilt correction algorithms, *Bound.-Lay. Meteorol.*, **99**, 127-150.